Effect of aluminium on polarization parameters and deposit characteristics in typical nickel sulfate electrolyte for electrowinning applications

Liezl Schoeman,[a,#] Emmanuel N. Nsiengani,[b] Kathryn C. Sole,[c,*] and Roelf Sandenbergh[d]

Department of Materials Science and Metallurgical Engineering, University of Pretoria,
Private Bag X20, Hatfield, Pretoria 0028, South Africa
[a]liezl.greeff.schoeman@gmail.com
[b]aim.nsanda@yahoo.com
[c]kathy.sole@up.ac.za
[d]roelf.sandenbergh@up.ac.za
* Corresponding author
# Current address: CSIRO Energy, Queensland Centre for Advanced Technologies, Pullenvale, Brisbane 4069, Australia

Highlights

- Effect of aluminium in electrolyte on nickel electrowinning was studied.
- Highly strained nickel deposits and decreased buffering resulted from electrolyte containing ≤1250 mg/L Al.
- Higher Al concentrations promoted desirable deposit morphology, reduced stress, and increased buffering.
- Higher Al concentrations gave comparable or better buffering performance than boric acid.

Abstract

Impurities present in the sulfate electrolyte during nickel electrodeposition influence the electrowinning process and morphology of deposited nickel metal in various ways. The presence of aluminium can be either detrimental or beneficial, depending on its concentration. Effects of the presence of aluminium in the electrolyte during nickel electrowinning were investigated by evaluation of the relationship between nucleation and plating overpotentials, nickel morphology, deposit contamination, internal stress development, and buffer characteristics of the electrolyte. Results showed that aluminium present at concentrations of lower than 1250 mg/L was unfavourable for the electrowinning process and highly strained nickel deposits of poor morphology were produced; at higher concentrations, the presence of aluminium was advantageous for the morphology and internal

stress, and correlated with increased buffer characteristics of the electrolyte.

Keywords
nickel electrowinning; aluminium impurity; deposit morphology; nucleation overpotential; plating overpotential, galvanodynamic polarisation; internal stress

Declarations of interest: None

1. Introduction

The process efficiency and product quality of nickel produced by electrowinning are highly dependent on electrowinning bath conditions, electrolyte concentrations, electrical operating parameters, and the presence of impurities and additives in the electrolyte. Optimisation and careful balance of the relationships between these parameters is crucial to obtaining nickel of the required purity specification and morphology characteristics (Holm and O'Keefe, 2000a; Crundwell et al., 2011). Electrodeposited nickel metal is generally associated with significant internal stress. High internal stress development during electrodeposition can often be attributed to impurities present in the feed electrolyte. Subsequent degradation of deposit quality, morphology, characteristics, and, in severe cases, even short circuits in the electrowinning cell are observed (Gogia and Das, 1991; Kittelty, 2002).

Many studies have been conducted to investigate the effects of typical impurities in sulfate electrolytes for nickel electrowinning applications. Most impurities behave similarly and are detrimental to various degrees (Gogia and Das, 1988, 1991; Holm and O'Keefe, 2000; Mohanty et al., 2005a). Tolerance limits for Cu^{2+}, Co^{2+}, and Fe^{2+} impurities in nickel electrolytes were found to be 100, 500, and 5 mg/L, respectively (Gogia and Das, 1991). These impurities co-deposit with nickel, incorporating into the crystal structure and thereby increase internal stress. Under these conditions, current efficiency is not severely influenced. Co^{2+}, Cu^{2+}, and Cr^{3+} were also found to incorporate into the nickel structure during electrodeposition and, even at concentrations as low as 20 mg/L, an increase in deposit strain was observed in their presence in the electrolyte (Nicol and Kittelty, 2001; Kittelty, 2002; Voogt et al., 2017). In the presence of Mg^{2+}, Mn^{2+}, or Zn^{2+} impurities, current efficiency does not change significantly, but the purity and especially the quality of nickel deposits

deteriorate considerably: tolerance limits of 100, 500, and 250 mg/L, respectively, were proposed (Gogia and Das, 1988).

Aluminium, however, shows somewhat anomalous behaviour in nickel electrowinning applications, depending on the conditions and its concentration in the electrolyte. Gogia and Das (1988) studied the effect of Al^{3+} up to a concentration of 100 mg/L in the presence of boric acid and sodium sulfate. Their results showed that nickel deposit contamination increased with increasing Al^{3+} concentration in the electrolyte. The current efficiency decreased in the presence of Al^{3+} and severe degradation of the nickel deposit morphology and quality was observed with 5 mg/L of Al^{3+} in the electrolyte. Contamination of the deposit and possible precipitation of hydroxides were proposed to be responsible for the degraded deposits.

Holm and O'Keefe (2000a, 2000b) studied the effect of Al^{3+} in nickel electrowinning from sulfate electrolytes in the absence of modifying agents and buffers. Serious degradation of the deposit morphology and current efficiency was observed with 20 mg/L to 100 mg/L Al^{3+} added to the electrolyte. Higher concentrations of approximately 1000 mg/L Al^{3+} decreased current efficiency and prevented deposition of metallic nickel, giving rise instead to a green–black layer on the cathode, identified as a mixed hydroxide, that might have allowed only significant hydrogen evolution. In contrast, the addition of 5000 mg/L Al^{3+} gave a smooth and compact nickel deposit without significant strain. It was proposed that Al^{3+} may contribute to the buffer capability of the system in a similar way to the action of boric acid or NH_4^+ ions.

Electrodeposition of nickel in the presence of Al^{3+} from sulfate solution containing 12 g/L of boric acid was potentiodynamically studied by Mohanty et al. (2005b) in the range of 0 to 40 mg/L Al^{3+}. An increase in aluminium content in the deposit with increased aluminium concentration in the electrolyte was observed. Deposit contamination was found to be related to a rise in surface pH due to increased hydroxide formation on the cathode surface. Significant deterioration of the deposit was observed as the concentration increased above 10 mg/L Al^{3+}. A shift to more negative potentials of galvanodynamic polarization diagrams in the presence of aluminium in the electrolyte was also related to the formation of hydroxide. Unfortunately, the experimental pH and temperature used in this work were not reported.

Nicol and Kittelty (2001), Kittelty (2002), and Kittelty and Nicol (2003) also studied the electrocrystallization of nickel and its relationship to the physical properties of the cathode product. The stress in nickel deposits was measured in terms of shear strain. These authors reported smooth deposits at high aluminium concentration (2700 mg/L Al^{3+}), which was related to an increase in pH buffer capacity of the electrolyte. The nickel morphology degraded at low (20–40 mg/L) Al^{3+} concentrations. It was proposed that at low Al^{3+} concentrations and as the bulk pH increases to around 4 as electrodeposition proceeds, Al^{3+} exists as $Al(OH)_3$, which increases the oxygen content of nickel electrodeposits due to co-deposition (Kittelty, 2002; Nicol and Kittelty, 2003). If Al^{3+} concentrations are much higher, predominant forms may include $Al_2(OH)_2^{4+}$ and $Al(OH)_2^{+}$. These complexes most likely buffer the electrolyte to keep the bulk pH constant and less than approximately pH 6, at which $Ni(OH)_2$ precipitates readily form. It was found that the bulk pH was more stable in the presence of higher Al^{3+} concentrations than in the presence of boric acid only. Therefore, under such conditions, aluminium is not expected to co-deposit with nickel and purer less-strained deposits were obtained (Kittelty, 2002; Nicol and Kittelty, 2003).

In our previous work (Schoeman and Sole, 2017a; Schoeman and Sole, 2017b), a two-step galvanodynamic measurement technique was developed to classify, monitor, and evaluate the effects of the presence of impurities and additives at various concentrations on the morphology and strain of nickel electrodeposits. The technique, adapted from the original concept proposed by Adcock and co-workers for zinc electrowinning (Adcock et al., 2002; Adcock et al., 2004; Adcock and Fraser, 2016), provides information regarding changes in nucleation and growth processes during the initial deposition of nickel onto a foreign substrate as a function of changes in the electrolyte composition. Results indicated that changes in polarisation parameters could be directly related to electrolyte composition and evolution of nickel morphology, quality, and strain in the presence of Co^{2+} and Cu^{2+} impurities. In the present work, this polarisation measurement technique was specifically applied to a wide range of Al^{3+} concentrations to formulate a more definitive understanding of the effects related to Al^{3+} impurity.

The baseline experimental conditions of this study were close to those of commercial nickel electrowinning operations (Crundwell et al., 2011) and the typical electrolyte used at Anglo American Platinum's Rustenburg Base Metal Refiners (South Africa) (Bryson et al., 2008; Voogt et al., 2017). These conditions were used as the reference point in our previous work

(Schoeman and Sole, 2017a; Schoeman and Sole, 2017b) for production of good quality nickel metal with low strain and desired morphological characteristics. In the present work, both low and high aluminium concentrations in the electrolyte were considered: a range of 10 mg/L to 5000 mg/L Al^{3+} was examined. The electrochemical analysis was correlated with measurements of stress in nickel deposited on a titanium substrate. These results, combined with visual observation, chemical analysis of deposits, and galvanodynamic polarisation measurements on the electrolytes, revealed that the stress may be attributed to the incorporation of aluminium (most probably as an oxide or hydroxide) impurity with nickel, with less incorporation occurring at higher aluminium concentration in the electrolyte as a consequence of improved buffer capacity.

Table 1. Electrolyte compositions and pH

Electrolyte description	Ni^{2+} (g/L)	Na_2SO_4 (g/L)	H_3BO_3 (g/L)	pH	Al^{3+} (mg/L)
Reference	80	80	4	3	0
Lower Ni^{2+}	**65**	80	4	3	0
	50	80	4	3	0
Higher H_3BO_3	80	80	**8**	3	0
	80	80	**12**	3	0
Higher pH	80	80	4	**3.5**	0
	80	80	4	**5**	0
Lower pH	80	80	4	**2**	0
No H_3BO_3	80	80	**0**	**5**	0
	80	80	**0**	**2**	0
Al^{3+} impurities	80	80	4	3	**5**
	80	80	4	3	**10**
	80	80	4	3	**300**
	80	80	4	3	**625**
	80	80	4	3	**1250**
	80	80	4	3	**2500**
	80	80	4	3	**5000**

2. Experimental

2.1. Overpotential measurements

Galvanodynamic polarisation measurements were carried out to measure the variations in nucleation and plating overpotentials with increasing aluminium concentration. An electrolyte without any impurities was used as the reference electrolyte: this comprised 80

g/L Ni^{2+} (supplied as the sulfate salt), 80 g/L Na_2SO_4, and 4 g/L H_3BO_3. Other electrolytes with varying Ni^{2+} and H_3BO_3 concentrations and variation in pH were prepared (Schoeman and Sole, 2017a; Schoeman, 2018). These were compared with electrolytes contining Al^{3+} (from the sulfate salt) concentrations varying across a wide range of three orders of magnitude. The electrolytes studied are indicated in Table 1.

All polarisation measurements were made using a three-electrode setup equipped with a titanium working electrode, a lead (0.1 % Ag) anode, and a Ag/AgCl (saturated KCl, at temperature) reference electrode. The anode and cathode were separated by an ion-permeable polyethylene membrane. The electrolyte temperature was controlled at 60 ± 1 °C using a water-jacketed vessel and the pH was maintained at 3.0 by adjusting with either 0.1 M NaOH or H_2SO_4. A two-step galvanodynamic method was used to measure the nucleation overpotential (E_n) on the slow forward scan and the plating overpotential (E_p) on the faster backward scan. The overpotentials are defined relative to the reference electrode with cathodic overpotentials taken as positive. The scan rates are shown in Table 2: the detailed experimental method can be found in our previous work (Schoeman and Sole, 2017a).

Table 2. Conditions of galvanodynamic method for measurement of *En* and *Ep*

Scan direction	Scan rate (mA s^{-1})
Scan 1: Cathodic 0 mA to −0.3 mA	0.1125
Scan 2: Cathodic −0.3 mA to −90 mA, then anodic −90 mA to 0 mA	0.5625

2.2. Morphological characteristics of nickel deposits

After polarisation measurements were made (as described in Section 2.1.), the potentiostat was set to automatically switch over to a programme to produce thicker nickel deposits. Cathodes with an exposed surface area of 2.25 cm^2 were used at 60 °C with each electrolyte by applying a constant current density of 220 A/m^2 for 2 h. The obtained deposits were stripped from the cathode surface and a cross-section was epoxy-mounted. The samples were sequentially polished using 400, 800, 1200, and 2400 grit paper, followed by 6 µm, 3 µm, and then <1 µm diamond paste to remove any scratches. The deposits were etched with 46 % nitric acid solution for 10 s, washed with deionised water, then dried in ethanol and air before using optical microscopy (Olympus, BX51M, Japan) to observe the microstructures. Typical characteristics used for morphological classification are indicated in Table 3 (Winand, 1991; Winand, 1994).

Table 3. Characteristics used for morphological classification of nickel electrodeposits

Morphological type	Characteristics observed
UD (Unoriented dispersion)	Fine grains, compact, no pinholes, grain size uniform, level, no peeling or strain cracks, no pitting
FT (Field oriented, textured)	Compact deposits, elongated grains, low strain, no peeling
BR/FI (Basis reproduction/Field orientated isolated crystals)	Loosely packed grains, pinholes, pitting, irregular structure and grain size, not level, strained, cracked

2.3. Internal stress and yield stress

Internal stress that developed during the plating of nickel from electrolytes containing various concentrations of aluminium was measured using a thin (0.75 mm) flexible titanium substrate as the cathode. This was clamped in a cantilever arrangement parallel to the anode, free on the side opposite the anode and isolated electrically on the other side using a silicone coating so that deposition could occur only on one side. As stress developed in the film that deposited onto the substrate during electrodeposition, the substrate and deposit bent together as a compound beam. The deflection was monitored using a linear variable differential transformer (LVDT) of high sensitivity (750 mV/mm at 10 V DC; Solartron, UK) as a transducer, coupled to a DataTaker DT 50 as signal conditioner, which detected the linear bottom substrate motion during deflection via a light and an electrically isolated rod pivoting around a well-lubricated fulcrum, the bottom of which linked to the substrate base in the cell and the top to the LVDT core tip outside the cell. A schematic of the experimental set-up used for the stress measurements is given in Figure 1. This design enabled in-situ stress development in a nickel deposit to be monitored in solution, while avoiding the risk of short circuits or an increase in bending resistance when using an immersed strain gauge or the need to know accurate elastic properties of the deposit (that could change with time during deposition) when using a shear strain method, for example.

The average internal stress (σ) in the plated nickel was calculated from deflection of the flexible cathode using the Stoney equation (Eqs. 1 and 2) (Stoney, 1909; Woo and Kim, 2011), where t_s refers to the substrate thickness (m), t_f is the film thickness (m), E_s is the substrate elastic modulus (MPa), v is Poisson's ratio of the substrate, K is the curvature of the cathode (1/m), δ is its deflection (m), and l_s is the substrate length (m):

$$\sigma = E_s K t_s^2 / [6(1 - v)t_f]; \quad (1)$$

$$K = 2\delta / l_s^2. \quad (2)$$

The film thickness was estimated using the mass of the deposit and the active plating area of 40 mm × 22 mm, considering a nickel density of 8.902 g/cm^3. The titanium substrate elastic modulus and Poisson's ratio were taken as 110 GPa and 0.28, respectively (Jorge et al., 2014).

Yield stress (σ_y) of the deposited nickel was calculated from the average observed grain size (d) determined by the intercept method on polished sections of the plated metal using the Hall–Petch relationship (Eq. 3) (Thompson, 1975; Carlton and Ferreira, 2007):

$$\sigma_y = \sigma_o + k/d^{1/2}, \quad (3)$$

where σ_o is the average intrinsic stress (MPa) for nickel and k is a mathematical constant (MPa.m$^{1/2}$) that is characteristic of the material. For all electrodeposits, values of 20 MPa and 0.16 MPa.m$^{1/2}$ were taken as the Hall–Petch constant for the average intrinsic stress σ_o and constant k, respectively, as found in previous work for pure nickel (Carlton and Ferreira, 2007; Armstrong, 2013; Armstrong, 2014) and assuming that the low levels of impurities investigated would not have a significant effect on these constants. The yield stress due to solid strengthening by the presence of the impurity was calculated using a nickel shear modulus and atomic radius of 76 GPa and 0.125 nm, respectively, but was found to be insignificant (typically less than 2%) when compared with the influence on the grain size (Nsiengani, 2017).

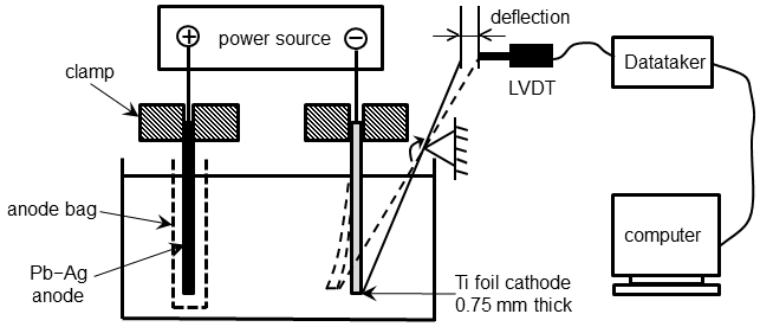

Figure 1. Schematic representation of experimental setup used for internal stress measurements in electrodeposited nickel

2.4. Aluminium contamination of deposit

Chemical analysis of the nickel deposits was determined in two ways. Firstly, a mounted sample of each deposit was analysed by scanning electron microscopy equipped with an

energy-dispersive x-ray spectrometer (SEM–EDS; Jeol, JSM-IT300, Japan) to determine the approximate mass percentage of each detected element. A sample of each deposit was also dissolved in 32 % HCl and quantitatively analysed by inductively coupled plasma optical emission spectroscopy (ICP–OES; Perkin Elmer, USA).

2.5. Buffer characteristics of electrolytes

Buffer characteristics of the electrolytes described in Section 2.1 were evaluated. A volume of 100 mL of each electrolyte was magnetically stirred on a hotplate, heated to 60 ± 1 °C, and the initial pH recorded with a calibrated benchtop pH meter (Orion 2-Star, Thermo Scientific, USA). A 0.1 M NaOH solution was then added in 0.5 mL aliquots and the pH of the solution was measured and recorded after each addition. Temperature was kept constant throughout all measurements at 60 ± 1 °C.

3. Results

3.1.1. Changes in polarisation parameters with increasing aluminium concentration

Changes in nucleation (E_n) and plating (E_p) overpotentials were measured with increasing aluminium concentration from 10 mg/L to 5000 mg/L Al^{3+}. The results are presented in Figure 2.

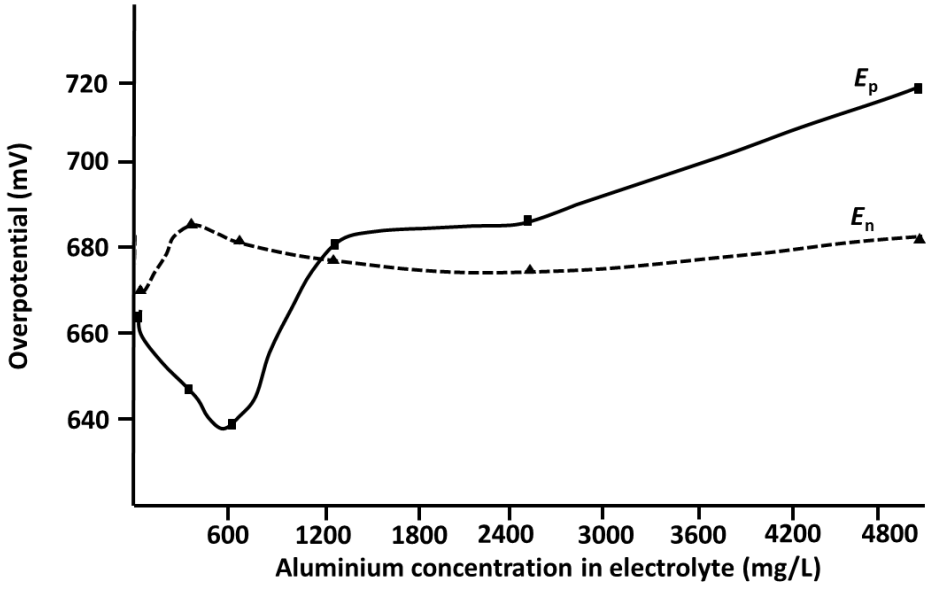

Figure 2. Relationship of E_n and E_p as a function of Al^{3+} concentration

An increase in Al^{3+} concentration had a more prominent effect on E_p than on the E_n values. At concentrations below 1250 mg/L Al^{3+}, E_p decreased to cathodic values well below the measured E_n values, which indicated an undesirable relationship between nucleation and growth for nickel electrodeposition (Andersen et al., 1985; Winand, 1991). Such a relationship is indicative of fast growth of large nickel crystallites without frequent nucleation of new nickel nuclei on the substrate surface: under such conditions, irregular large growths and poor morphology are expected (Andersen et al., 1985; Winand, 1991; Adcock et al., 2002; Adcock et al., 2004). At Al^{3+} concentrations above 1250 mg/L, the relationship between E_p and E_n shifted favourably and to values comparable with that of the reference electrolyte. Under these conditions, frequent nucleation of new nickel nuclei is promoted simultaneous to growth of already deposited atoms and therefore a fine-grained compact deposit is predicted (Andersen et al., 1985; Winand, 1991; Adcock et al., 2002; Adcock et al., 2004).

3.1.2. Comparison of polarisation parameters with variation in electrolyte composition

The difference between E_n and E_p (or ΔE) was calculated for each electrolyte and plotted against $-E_p$. This relationship is shown in Figure 3. Theoretically, if E_p is more cathodic than E_n (ΔE is positive), then three-dimensional nucleation and simultaneous growth are promoted, grains are more refined, and deposits with UD-type morphology predominate. As E_p becomes more negative, growth is promoted and levelling increases. Full descriptions of development of this methodology can be found in Adcock et al. (2002, 2004) and specifically with application to nickel electrowinning in our previous work (Schoeman and Sole, 2017a; Schoeman and Sole, 2017b; Schoeman, 2018).

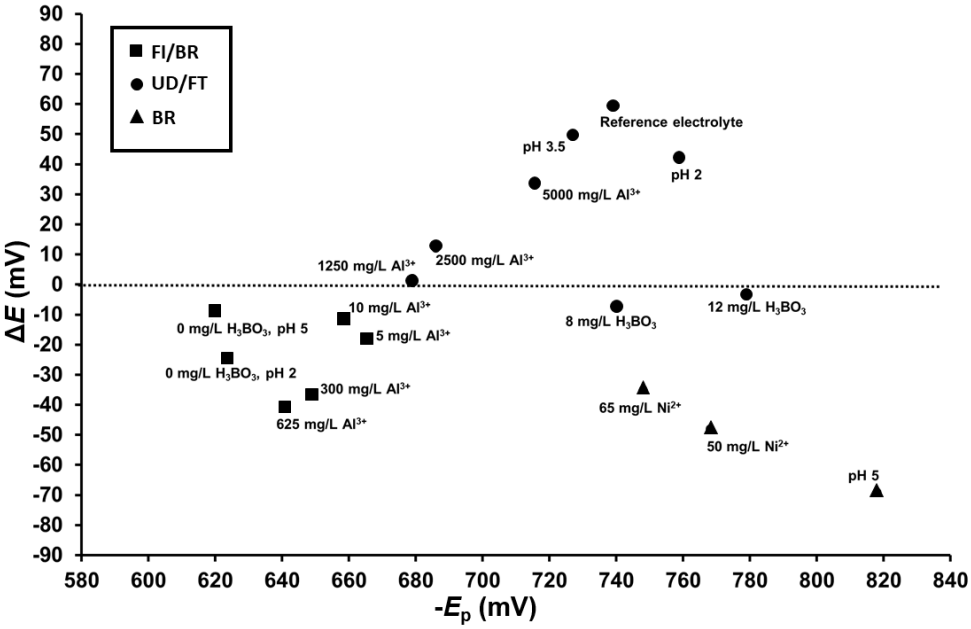

Figure 3. Comparison of polarisation parameters of electrolytes and resulting deposit morphology with varying electrolyte composition

Electrolytes with negative ΔE values and low cathodic E_p values included two electrolytes without H_3BO_3 (at pH 2 and pH 5) and several with low concentrations of Al^{3+} impurities (ranging from 5 mg/L to 625 mg/L). This relationship predicts infrequent nucleation and fast growth rates and therefore the morphology of the resulting deposits was of FI/BR type with some FT characteristics in the initially deposited layers.

Electrolytes with negative ΔE values and more cathodic E_p values included those with low Ni^{2+} concentrations, a high pH of 5, and the two increased concentrations of H_3BO_3. The morphologies of the low Ni^{2+} and pH 5 electrolytes were similar and of BR type. The morphologies of deposits from the 8 and 12 g/L H_3BO_3 electrolytes was of UD/FT type and comparable with those of the reference electrolyte and other electrolytes with positive ΔE values. Growth is promoted at more cathodic E_p values and proceeds faster than nucleation processes, so BR-type deposits are therefore expected.

The most desirable relationship between ΔE and E_p was obtained for the following electrolytes: the reference electrolyte, those with pH values of 2 and 3.5, and 5000 mg/L of Al^{3+} added to the electrolyte. This relationship is indicative of frequent three-dimensional nucleation simultaneous to adequate growth, and predicts morphologies of the most desirable

UD type. Deposits from these electrolytes were fine-grained, compact, level, and regular, and no internal stress was observed.

The electrolytes containing 1250 mg/L and 2500 mg/L Al^{3+} produced deposits with similar morphologies to that of deposits produced from the reference electrolyte. The ΔE values were positive and the $-E_p$ values were lower, but this relationship was still adequate to produce deposits of good morphology and low strain. In previous work (Schoeman and Sole, 2017a; Schoeman, 2018), we referred to this as an intermediate region, in which the relationship between E_n and E_p was still desirable and good morphologies with low strain were observed. Electrolytes with higher boric acid concentrations (8 g/L and 12 g/L H_3BO_3) had $-E_p$ values similar to that of the reference electrolyte, but slightly negative ΔE values. The morphologies of deposits from these electrolytes were very similar to that of the reference electrolyte and showed no signs of stress. It is assumed that, even at slightly lower nucleation, the relationship was nevertheless balanced in such a way that compact fine-grained morphologies were still prevalent.

The polarisation relationship data also showed an interesting trend. With increasing Al^{3+} concentration from 0–625 mg/L to 1250, 2500, and 5000 mg/L, the polarisation relationship shifted towards that of the reference electrolyte (Figure 3). As $-E_p$ increased, ΔE also increased with increasing Al^{3+} concentration from 1250 mg/L to 5000 mg/L, with the relationship data point for 5000 mg/L Al^{3+} slightly lower than that of the reference electrolyte.

3.2. Morphology and deposit characteristics

The nature of electrodeposited nickel plated from the aluminium-containing electrolytes is shown in Figure 4. Debonding from the titanium substrate at intermediate aluminium concentrations is clearly indicated. Morphologies of the thick nickel electrodeposits under various conditions are shown in Figure 5.

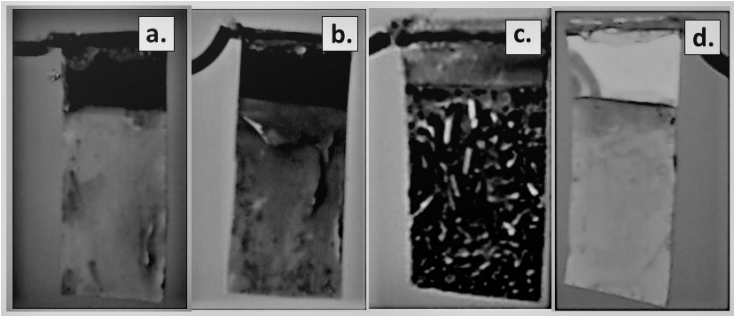

Figure 4. Visual appearance of nickel electrodeposits obtained from electrolytes with varying Al^{3+} concentrations: a. reference electrolyte; b. 5 mg/L Al^{3+}; c. 325 mg/L Al^{3+}; d. 2500 mg/L Al^{3+}

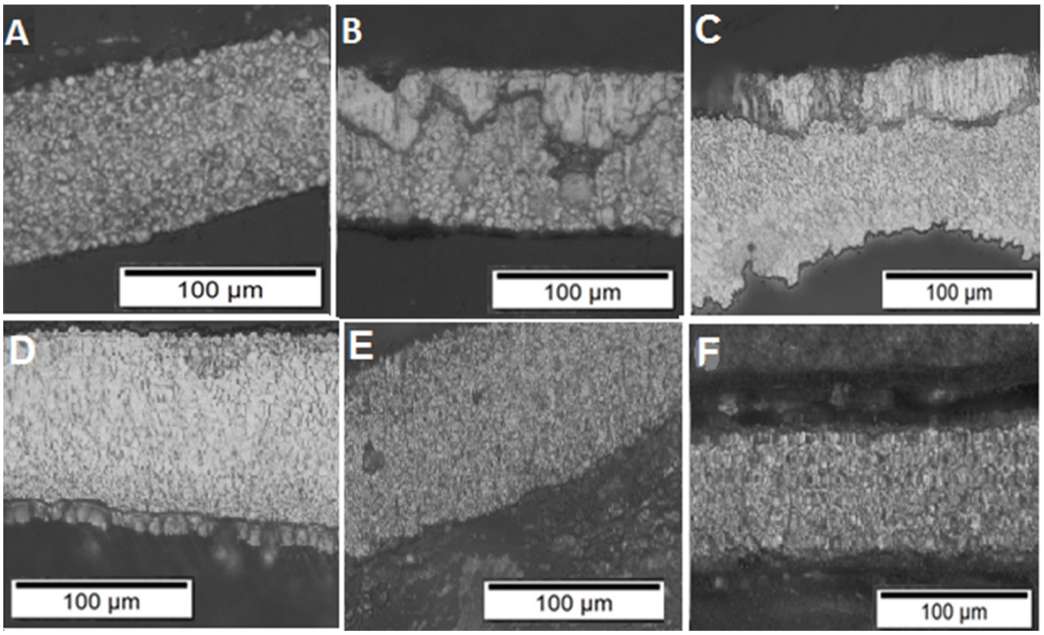

Figure 5. Morphologies obtained for deposits from various electrolytes (substrate is at the top of each photograph): A. reference electrolyte; B. 10 mg/L Al^{3+}; C. 600 mg/L Al^{3+}; D. 1250 mg/L Al^{3+}; E. 2500 mg/L Al^{3+}; F. 5000 mg/L Al^{3+}

Smooth low-stress deposits were obtained for the reference electrolytes without any Al^{3+} (Figure 4a) and with the addition of 2500 mg/L of Al^{3+} (Figure 4b). The characteristics of these deposits were similar, with good adherence to the substrate surface, level and bright appearance, and having overall desirable quality. In fact, the strain seemed to be lower at this high concentration of Al^{3+} when compared with that of the reference electrolyte. This showed that a high concentration of Al^{3+} was beneficial to mitigating stress development during nickel electrodeposition and confirmed that, under these conditions, a deposit with low strain, a more regular nickel structure, and lower aluminium contamination was produced. This

result is consistent with observations reported in previous studies (Nicol and Kittelty, 2001; Kittelty, 2002; Schoeman, 2018).

3.3. Internal stress development and deposit contamination

Table 4 compares the measured aluminium contents in nickel deposits obtained from two different analytical techniques: SEM–EDS and ICP–OES. Both techniques showed a decrease in nickel deposit contamination with increase in Al^{3+} concentration in the electrolyte from 300 mg/L to 2500 mg/L. The slight differences observed for the measurements recorded by the two techniques are attributed to their respective method sensitivities and detection limits.

Table 4. Relationship between aluminium content in the electrolyte and the resulting aluminium content in the nickel electrodeposits

$[Al^{3+}]$ in nickel electrolyte (mg/L)	Al in nickel electrodeposit (mass %)	
	SEM–EDS	ICP–OES
300	1.2	1.56
625	0.1	0.06
2500	0.0	0.01

A comparison of yield stress and internal stress with aluminium contamination measured in the nickel electrodeposit is shown as a function of aluminium concentration in the electrolyte in Figure 6.

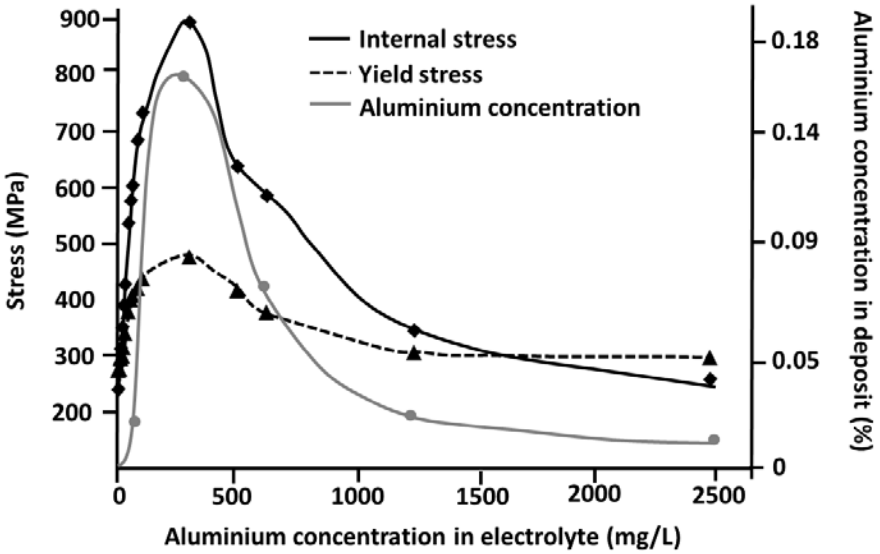

Figure 6. Comparison of internal and yield stresses with aluminium contamination for nickel deposits

Internal stresses calculated from the experimental data for each electrolyte were compared with the theoretically calculated yield stresses. High internal stresses were measured for nickel deposits produced in the presence of low concentrations of Al^{3+} in the electrolyte (< 1250 mg/L Al^{3+}), with a maximum in stress for the electrolyte that contained 300 mg/L Al^{3+}. Good quality deposits of desirable morphology and low strain were only obtained when the internal stress did not exceed the yield stress. In cases where internal stress exceeded the yield stress, rupture, peeling, and/or debonding of the deposit would occur. The desirable relationship and consequent low-strained deposits were only obtained from electrolytes containing 1250 mg/L Al^{3+} and higher.

Aluminium contamination in the nickel electrodeposits produced under these conditions (< 1250 mg/L Al^{3+} in the electrolyte) was also the highest. At higher concentrations of Al^{3+} in the electrolyte (≥ 1250 mg/L), internal stress decreased, and the aluminium contamination of the nickel electrodeposit similarly declined. It is evident that there is a strong correlation between stress in the deposit and the degree of aluminium contamination during nickel electrodeposition. Furthermore, this effect was pronounced only within a limited range of Al^{3+} impurity concentrations in the electrolyte; outside of this range, the presence of Al^{3+} in the electrolyte exerted negligible effect.

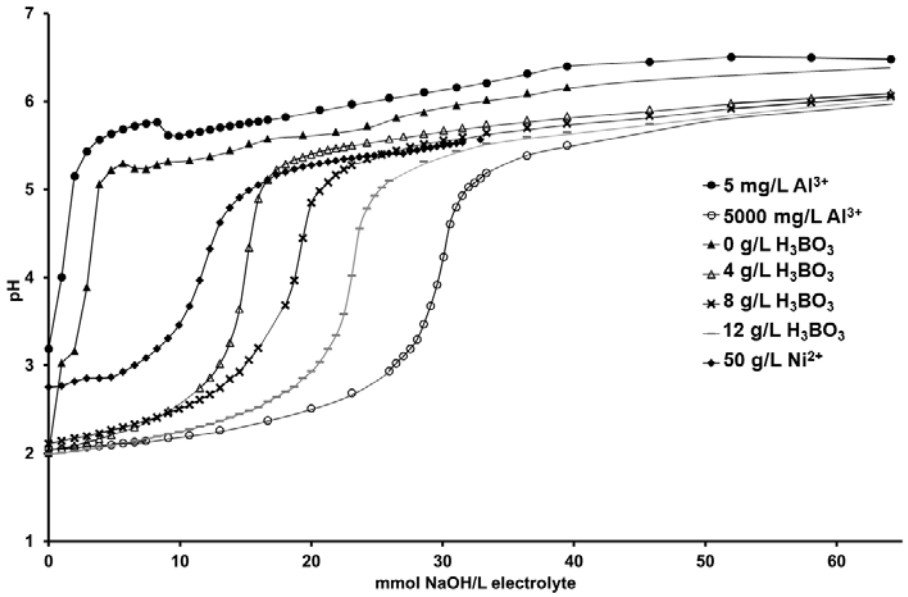

Figure 7. Measurement of pH as a function of increasing NaOH concentration in various electrolytes. The 4 g/L H_3BO_3 electrolyte refers to the standard reference electrolyte

3.4. Buffer characteristics of electrolytes

Figure 7 shows a comparison of the buffer capacity of various electrolytes with and without Al^{3+} impurities, with increasing H_3BO_3 concentration, and one with a lower Ni^{2+} concentration of 50 g/L.

The results show that low Al^{3+} impurity, even present as low as 5 mg/L, had detrimental effects on the buffering of the electrolyte. The pH of these electrolytes increased quickly upon the first few additions of NaOH to values at which $Ni(OH)_2$ can form and incorporate into the deposit. The electrolyte without H_3BO_3 also showed poor buffer capacity and behaved similarly. The buffer capacity of the electrolyte with low nickel concentration was also undesirable. These results therefore show that high concentrations of nickel and H_3BO_3 and the absence of Al^{3+} promote buffering of the system. The electrolytes with increasing H_3BO_3 concentration from 4 g/L (reference electrolyte) to 8 g/L to 12 g/L showed a corresponding increase in buffer capacity. The electrolyte with the best buffer capacity was found to be that containing 5000 mg/L Al^{3+}. This confirmed that, at high Al^{3+} concentrations, Al^{3+} could be even more advantageous to buffering the solutions than H_3BO_3. A similar result was reported by Kittelty (2002) and Nicol and Kittelty (2003) for an Al^{3+} concentration of 2700 mg/L; other concentrations were not investigated.

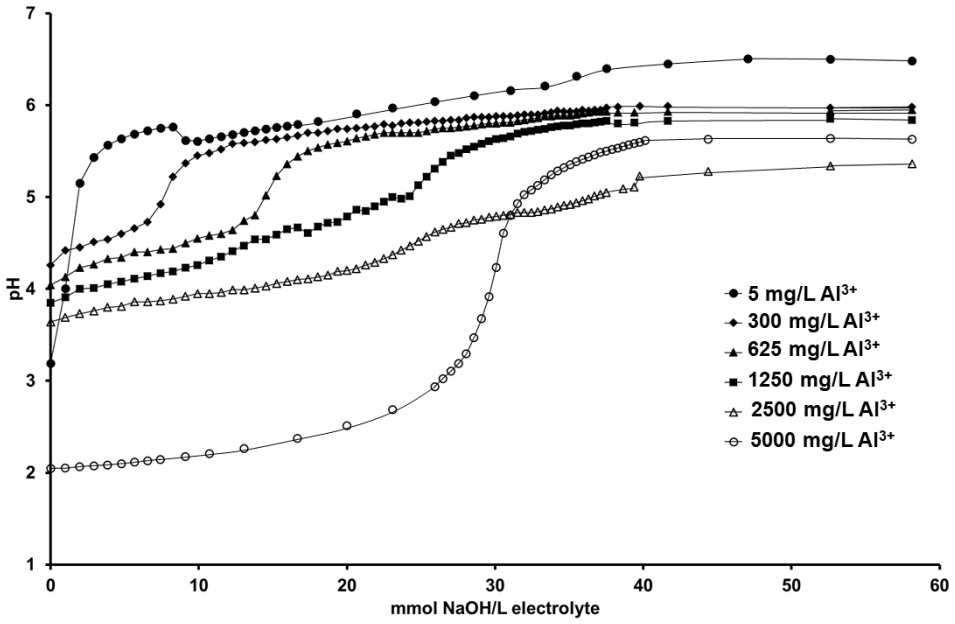

Figure 8. Measured pH as a function of increasing NaOH concentration in electrolytes with increasing Al^{3+} concentrations. These electrolytes all contained 4 g/L H_3BO_3

To determine the concentration at which the buffer capacity shifted from detrimental to advantageous, a series of electrolytes with increasing Al^{3+} concentrations were potentiometrically titrated against NaOH, as shown in Figure 8.

Results clearly show that buffer capacity of the nickel electrolyte increased with increasing Al^{3+} concentration. The buffer capacity of the electrolyte with 2500 mg/L Al^{3+} seemed to be the highest because the pH stayed most constant over the range of NaOH concentrations added and the pH did not increase to values above 5. The electrolyte with the highest Al^{3+} concentration of 5000 mg/L showed the most buffering of the solution for the initial additions of NaOH to the electrolyte and an even lower starting pH of the electrolyte was observed.

4. Discussion

The presence of Al^{3+} as an impurity in a nickel sulfate electrolyte significantly changes the electrodeposition behaviour, stress development, purity, and morphology of the deposited nickel. Polarisation behaviour indicated that both nucleation and growth of the nickel deposit were influenced by Al^{3+} concentration. Frequent nucleation of nickel simultaneous to growth of previously deposited nickel was observed for the reference electrolyte (no Al^{3+}) and at high concentrations of Al^{3+} (1250, 2500, and 5000 mg/L). Judging by the observed changes in nucleation and plating overpotentials, Al^{3+} impurities influenced growth processes of nickel more than nucleation. At concentrations above 1250 mg/L Al^{3+}, the relationship between nucleation and growth was similar to that of electrolytes without Al^{3+}.

This polarisation relationship was demonstrated to be indicative of developing internal stress. Comparison of Figures 3 and 6 clearly shows that internal stress and aluminium contamination increased with negative ΔE values. At concentrations of 1250 mg/L Al^{3+} and higher in electrolytes, positive ΔE values were measured, and aluminium precipitation and stress development decreased.

Internal stress in nickel deposits increased with increasing Al^{3+} concentration up to a limit of approximately 1250 mg/L Al^{3+}; at higher concentrations, the internal stress decreased to below the value of the yield stress. Internal stresses in excess of the yield stress caused delamination of the electrodeposited nickel; deposits were also cracked, irregular in morphological structure, and pin-holed. These effects were proportional to the aluminium

content measured in the nickel deposit. Therefore, in the presence of Al^{3+} in the electrolyte up to a concentration of 1250 mg/L, deposit contamination and internal stress were relatively higher and increased with increasing Al^{3+} concentration; at higher concentrations, the stress and deposit contamination decreased with increasing Al^{3+} concentration. Similar observations were reported by Kittelty (2002) and Nicol and Kittelty (2003).

Morphologies of deposits produced from electrolytes with 5000 mg/L Al^{3+} were fine-grained, level, uniform in structure, compact, and were similar in characteristics to deposits produced under optimised conditions without any impurities. The relationship between nucleation and plating (growth) was examined: frequent nucleation simultaneous with growth was prevalent at 5000 mg/L Al^{3+} in the electrolyte. This is the ideal outcome, and produced desired morphology and quality nickel electrodeposits with negligible contamination and strain.

Buffer capacity of the nickel electrolytes changed with Al^{3+} concentration within the three-orders-of-magnitude experimental range considered. Within the working pH range for nickel electrodeposition, the highest buffer capacities were measured for the reference electrolyte and those containing 1250 mg/L, 2500 mg/L, and 5000 mg/L Al^{3+}. This suggests that nickel, boric acid, and aluminium concentrations play major roles in the buffer capacity of these electrolytes and that optimisation of these are important to produce nickel deposits of desirable morphology and low strain.

The fact that higher aluminium concentrations were detected in nickel electrodeposits produced from electrolytes with low Al^{3+} impurities suggested that contamination of the deposits occurred by precipitation of aluminium during electrodeposition. The most probable mechanism of aluminium contamination is by formation and precipitation of $Al(OH)_3$, as suggested by Kittelty (2002) and Nicol and Kittelty (2003). In our analyses, however, we could not detect the presence of oxygen that would confirm this and we assume that our EDS capability was insufficiently sensitive.

5. Conclusions

The effect of aluminium as an impurity in nickel sulfate electrolyte on the characteristics of the resulting nickel electrodeposit was investigated under commercial nickel electrowinning conditions. The following conclusions were drawn:

- The effect of Al^{3+} impurities during nickel electrowinning from sulfate electrolyte is strongly dependent on the Al^{3+} concentration.
- At concentrations below 1250 mg/L, Al^{3+} is detrimental to nickel electrodeposition and influences the stress development and morphology of the nickel electrodeposit crystal structure.
- At concentrations above 1250 mg/L, Al^{3+} is beneficial to the nickel electrodeposition process, reduces stress development, and is correlated with stimulating frequent nucleation of new nickel crystals while growth of already-deposited crystals occurs.
- High concentrations of Al^{3+} allowed maintenance of the working pH of the electrolyte, thereby apparently stabilising the nickel electrodeposition process. Polarisation measurements of nucleation and growth processes as well as pH measurements were found to be systematically sensitive to the presence and concentration of Al^{3+} impurities.

Although all of the data presented in this study from different experimental techniques are self-consistent, the mechanistic reasons for the effects attributed to changes from low to intermediate to high Al^{3+} concentrations in the electrolyte are still not fully understood. These are likely due to changes in speciation of Al^{3+} compounds close to the cathode surface, and remain a topic for further investigation. Nevertheless, these results shed some light on the behaviour and impact of Al^{3+} in a nickel electrowinning system from sulfate electrolyte and can be useful in understanding effects in industrial processes where Al^{3+} may be present as a contaminant from upstream processes.

Acknowledgements

This work was partially supported by the Industrial Metals and Minerals Research Institute (IMMRI) based at the University of Pretoria. Anglo American Platinum Rustenburg Base Metals Refiners is acknowledged for providing samples, suggestions, and technical support. We thank Ruzanne Engelbrecht for assistance with confirmatory experimental work. We are also grateful for the insightful and valuable comments of two anonymous reviewers based on an earlier version of this manuscript.

References

Adcock, P.A., Fraser, R.J., 2016. Nucleation overpotential and the role of nucleation early and late in a deposition cycle. International Minerals Processing Congress 2016

Proceedings, Canadian Institute of Mining, Metallurgy and Petroleum, Montreal, Canada. Paper #274.

Adcock, P.A., Adeloju, S.B., Newman, O.M.G., 2002. Measurement of polarization parameters impacting on electrodeposit morphology I: Theory and development of technique. J. Appl. Electrochem., 32, 1101–1107.

Adcock, P.A., Quillinan, A., Clark, B., Newman, O.M.G., Adeloju, S.B., 2004. Measurement of polarization parameters impacting on electrodeposit morphology. II: Conventional zinc electrowinning solutions. J. Appl. Electrochem., 34, 771–780.

Andersen, T.N., Kerby, R.C., O'Keefe, T.J., 1985. Control techniques for industrial electrodeposition from aqueous solutions. J. Met., 36–43.

Armstrong, R.W., 2013. Hall-Petch analysis of dislocation pileups in thin material layers and in nanopolycrystals. Mater. Res. Soc., 28, 13, 1792–1798.

Armstrong, R.W., 2014. 60 Years of Hall-Petch: past to present nanoscale connections. Mater. Trans., 55, 1, 2–12.

Bryson, L.J., Graham, N.J., Bogosi, E.P., Erasmus, D.L., 2008. Nickel electrowinning tank house developments at Anglo Platinum's Base Metal Refinery. ALTA Ni/Co 2008, ALTA Metallurgical Services, Melbourne, Australia.

Carlton, C.E., Ferreira, P.J., 2007. What is behind the inverse Hall-Petch effect in nanocrystalline materials? Acta Mater., 55, 11, 3749–3756.

Crundwell, F.K., Moats, M.S., Ramachandran, V., Robinson, T.G., Davenport, W.G., 2011. Extractive Metallurgy of Nickel, Cobalt and Platinum-Group Metals. Elsevier. pp. 327–346.

Duarte, H.M.S., Belinha, J., Dinis, L.M.J.S., Jorge, R.M.N., 2014. Analysis of a bar-implant use a meshless method. In Biodental Engineering II, Jorge, R.M.N., Campos, J.C.R., Tavares, J.M.R.S., Vaz, M.A.P., Santos, S.M. (eds.), CRC Press, London. pp. 139–144.

Gogia, S.K., Das, S.C., 1988. The effects of Mg^{2+}, Mn^{2+}, Zn^{2+}, and Al^{3+} on the nickel deposit during electrowinning from sulfate bath. Met. Trans. B, 19B, 823–831.

Gogia, S.K., Das, S.C., 1991. The effect of Co^{2+}, Cu^{2+}, Fe^{2+} and Fe^{3+} during electrowinning of nickel. J. Appl. Electrochem., 21, 64–72.

Holm, M., O'Keefe, T.J., 2000a. Electrolyte parameter effects in the electrowinning of nickel from sulfate electrolytes. Miner. Eng., 13, 2, 193–204.

Holm, M., O'Keefe, T.J., 2000b. The anomalous behaviour of Al^{3+} in nickel electrowinning from sulfate electrolytes. Metall. Mater. Trans. B, 31B, 2000–2003.

Kittelty, D., 2002. The electrocrystallization of nickel and its relationship to the physical properties of the metal. PhD thesis, Murdoch University, Australia.

Kittelty, D. and Nicol, M.J., 2003. The effects of solution impurities on the properties of nickel cathodes. Hydrometallurgy 2003, Proceedings of the 5th International Symposium, Vol. 2. Young, C. Alfantazi, A., Anderson, C., James, A. Dreisinger, D., Harris, B. (eds.). The Minerals Metals and Materials Society, Warrendale, PA, USA. pp. 1205–1217.

Küzeci, E., Kammels, R., Gogia, S.K., 1994. Effects of metallic and D2EHPA impurities on nickel electrowinning from aqueous sulphate baths. J. Appl. Electrochem., 24, 730–736.

Mohanty, U.S., Tripathy, B.C., Singh, P., Das, S.C., Misra, V.N., 2005a. Effect of pyridine and picolines on the electrocrystallization of nickel from sulphate solutions. Surf. Coat. Technol., 197, 247–252.

Mohanty, U.S., Tripathy, B.C., Singh, P., Das, S.C., Misra, V.N., 2005b. Electrodeposition of nickel in the presence of Al^{3+} from sulfate baths. J. Appl. Electrochem., 35, 545–549.

Nicol, M.J., Kittelty, D., 2001. The electrocrystallisation of nickel and its relationship to the physical properties of the metal. Electrometallurgy 2001, Canadian Institute of Mining, Metallurgy and Petroleum, Montreal, Canada, pp. 361–374.

Nsiengani, E.N., 2017. Effect of impurities in a nickel sulfate electrolyte on internal stress development, morphology and adhesion to titanium of electrodeposited nickel. Master of Applied Sciences Dissertation, University of Pretoria, South Africa. Available from https://repository.up.ac.za > bitstream > handle > Nsiengani_Effect_2017.

Schoeman, L., 2018. Evaluation of polarisation parameters as predictor of morphology of nickel electrodeposits produced from sulfate electrolyte. PhD Thesis, University of Pretoria, South Africa. Available from https://repository.up.ac.za > bitstream > handle > Schoeman_Evaluation_2018.

Schoeman, L., Sole, K.C., 2017a. Prediction of morphology development from nucleation and plating overpotentials in nickel electrodeposition. Can. Metall. Quart., 56, 4, 393–400.

Schoeman, l., Sole, K.C. (2017b). Accurate measurement of polarization potentials during electrodeposition of nickel metal from sulphate electrolytes. J. S. Afr. Inst. Min. Metall., 117 (7), 623–628.

Stoney, G.G., 1909. The tension of metallic films deposited by electrolysis. Proc. Royal Soc. London, Ser. A, 82, 553, 172–175.

Thompson, A.W., 1975. Yielding in nickel as a function of grain or cell size, Acta Metall., 23, 11, 1337–1342.

Voogt, K., Brits, J.H.W.M., Bryson, L., 2017. Stress in full deposit electrowon nickel. Proceedings Conference of Metallurgists CIM/COM 2017, Canadian Institute of Mining, Metallurgy and Petroleum, Montreal, Canada. Paper #9691.

Wilson, K., Walker, K., 2000. Practical Biochemistry, fifth ed., Cambridge University Press, United Kingdom, pp. 37–42.

Winand, R., 1991. Electrocrystallization: fundamental considerations and application to high current density continuous steel sheet plating. Rev. Appl. Electrochem., 27, 377–385.

Winand, R., 1994. Electrodeposition of metals and alloys – new results and perspectives. Electrochim. Acta, 39, 8/9, 1091–1105.

Woo, Y., Kim, S., 2011. Sensitivity analysis of plating conditions on mechanical properties of thin films for MEMS applications. J. Mech. Sci. Technol., 25, 4, 1017–1022.